Journal of Coastal Research	23	4	1015–1027	West Palm Beach, Florida	July 2007

Hydrodynamics and Associated Morphological Variations on an Estuarine Intertidal Sand Flat

Yusuke Uchiyama*

Littoral Drift Division
Port and Airport Research Institute
Yokosuka 239-0826, Japan

ABSTRACT

UCHIYAMA, Y., 2007. Hydrodynamics and associated morphological variations on an estuarine intertidal sand flat. *Journal of Coastal Research,* 23(4), 1015–1027. West Palm Beach (Florida), ISSN 0749-0208.

Hydrodynamics, sediment suspension, and morphological response on an estuarine intertidal sand flat in Tokyo Bay, Japan, are examined through a field experiment performed for 16 days in winter 2000 and using a bathymetry data set based on a 6-year series of surveys. Topography of the sandy flat was found to fluctuate by approximately 8 cm during the deployment, while the long-term accumulation rate is estimated with the surveyed bathymetries to be only 3.8 cm/y. Cross-spectral analysis of the measured data indicates that on the sandy tidal flat, semidiurnal or shorter-period fluctuations in current velocity are mostly attributed to semidiurnal tides and waves, whereas wind above the sea generally drives diurnal or longer-period fluctuations. The field data also confirm that suspended sediment concentrations were highly correlated with bed shear stress, which is generated by combination of tidal current, wind-induced current, and wind waves. Episodic erosion is observed on the sandy flat with high turbidities on ebbing phases. Erosion evidently occurs at phases between the high slack and the mean tidal levels during ebb flows when combined tidal, wind-driven, and wave-driven currents are maximized.

ADDITIONAL INDEX WORDS: *Wetting and drying, topography change, bed shear stress, tidal oscillation, wind waves, wind-induced current.*

INTRODUCTION

For preservation and rehabilitation of ecosystems on tidal flats, wetlands and salt marshes, predicting morphological behavior is a significant issue (PATERSON, 1989). The intertidal sediments play a key role in providing habitat for resident infauna, which act as a food resource for large communities of shorebirds (FERNS, 1983; BAKKER *et al.,* 1993). Even when slight erosion occurs on tidal flats, it may have significant impact on the resident benthos (KAKINO, 2000). Understanding of the hydrodynamics and associated morphological process on intertidal flats and wetlands is a prerequisite for the development of conceptual and quantitative models that are essential to allow effective management of the intertidal area.

Recently, efforts have been made to understand hydrodynamics, sediment transport, and resultant morphological process on mudflats located in the Dollard Estuary, the Netherlands (DYER *et al.,* 2000; VAN DER LEE, 2000), Humber Estuary, UK (CHRISTIE *et al.,* 1999), Severn Estuary, UK (O'BRIEN *et al.,* 2000), Baie de Marennes-Oleron, France (BASSOULLET *et al.,* 2000), the Wadden Sea, the Netherlands and Denmark (HOUWING, 2000; ANDERSON, 2001; ANDERSON and PEJRUP, 2001), and San Francisco Bay, USA (TALKE and STACEY, 2003). Sedimentological processes reported in these studies have usually been described in comparison with laboratory data (TEISSON *et al.,* 1993), and there is a growing literature on the influence of mixtures of various sizes of sediments (*e.g.,* MITCHENER *et al.,* 1996; TORFS *et al.,* 1996) and biological factors (*e.g.,* RHOADS and BOYER, 1982; PATERSON, 1989; WIDDOWS *et al.,* 1998; AUSTEN *et al.,* 1999; ANDERSON, 2001). Furthermore, AMOS *et al.* (1988) have documented that the subaerial exposure often has considerable influence on bed strengthening. Some studies have examined hydrodynamics that potentially control sediment transport and morphological process on mudflats by measuring tidal currents, wind-induced currents, wind waves, oceanic swells and infragravity waves, density-driven circulation, and drainage processes (*e.g.,* LE HIR *et al.,* 2000; TALKE and STACEY, 2003).

Sediment transport on tidal flats occurs over a variety of time scales, ranging from seconds to seasons. DALRYMPLE *et al.* (1991), in a paper on cohesive sediment deposition on a mudflat in the Bay of Fundy, indicate that historical deposition may be divided into two phases, namely, a short-term rapid erosion and subsequent aggradation, and longer-term gradual but quasiequilibrium topographic fluctuations. They also reported that deposited sediments are intensely disturbed by benthic organisms. The combination of morphological processes in different time scales may control overall development of intertidal areas. Intertidal topographic variations have been reported to be generally minor as hydrodynamic forcing has basically been observed to be small in previous studies (*e.g.,* CHRISTIE *et al.,* 1999). For example, KIRBY *et al.* (1993) demonstrated that bed elevation varies only 3–5 cm a year in Strangford Lough, Northern Ireland. How-

DOI:10.2112/04-0336.1 received 26 August 2004; accepted in revision 18 May 2005.

* Present address: Institute of Geophysics and Planetary Physics, University of California, Los Angeles, 3845 Slichter Hall, Los Angeles, CA 90095-1567, U.S.A. uchiyama@atmos.ucla.edu.

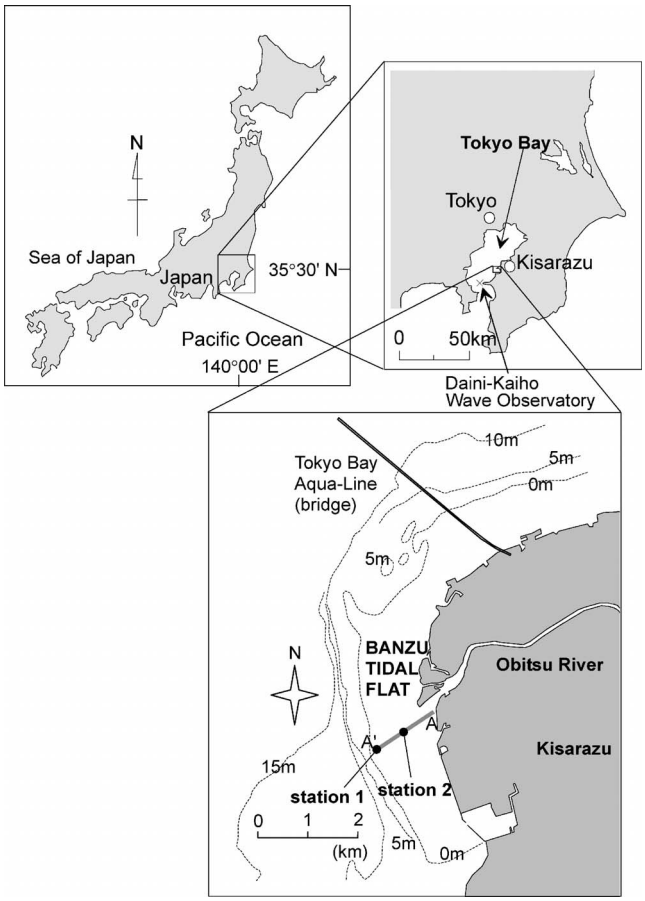

Figure 1. The location of Banzu intertidal sand flat, Tokyo Bay, Japan. Bed profiles were surveyed along transect A–A′ in the vicinity of the Obitsu River mouth.

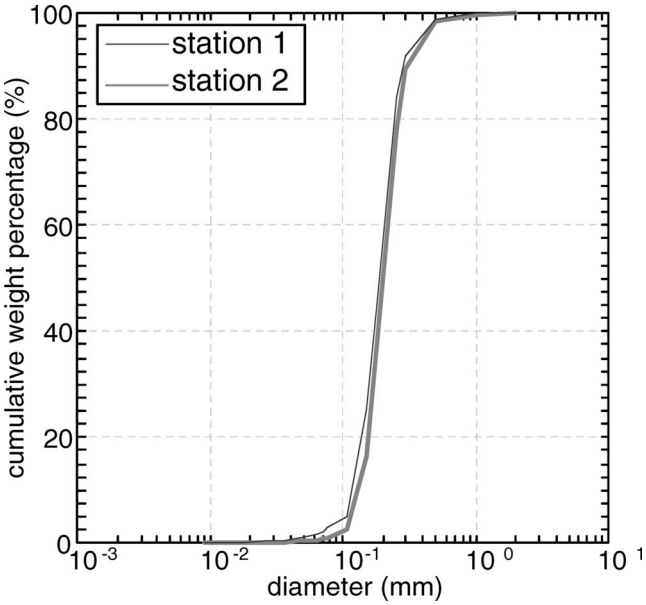

Figure 2. Grain size distributions of bottom sediments sampled at stations 1 and 2. Median grain sizes are estimated to be 170–190 μm.

ever, intermittent episodic processes are considered to dominate the morphodynamics on intertidal areas. Storms can produce significant sediment transport and cause topographic changes that are likely to occur for several years without storms. Episodic fluvial outflows can also induce significant accretion. Recent studies have reported that considerable short-term morphological variations of 10–30 cm on a mudflat in the Severn Estuary (WEST and WEST, 1991; WHITEHOSE and MITCHENER, 1998; O'BRIEN *et al.,* 2000). Therefore, morphological processes on intertidal flats, not only in the long term but also in the short term, provide an "open" question.

Intertidal flats are characterized by tidal submergence-emergence cycles with the additional effect of benthic disturbance and exposure to the air. The fluctuations in water surface elevation induce hydrodynamic conditions that generate sediment processes such as formation of ripples, dunes, channel networks, and so on. These external forces are responsible for sediment transport through producing bed shear stresses affected by nonlinear wave-current interaction and are attributed to erosion and accretion of the bed.

The purpose of the present study is to demonstrate short- and long-term morphological behavior of a sandy tidal flat rather than mudflats reported in the previous studies. The prime objective is to investigate episodic (short-term) and gradual (long-term) morphological processes on the sandy flat, to investigate mechanisms of erosion related to estimating bed shear stresses caused by combined effects of waves and currents, and to examine detailed hydrodynamics, sediment suspension, and associated morphodynamic processes in contrast to long-term topography variations. Biological effects on sediment suspension and subaerial exposure are neglected in the present study but should be considered in future works.

FIELD MEASUREMENT

Study Site

Field measurements were carried out for 16 days, February 7–22, 2000, on an intertidal sandy flat at Banzu situated on the eastern shore of Tokyo Bay, Japan (Figure 1). This embayment is characterized by a well-mixed semidiurnal mesotidal condition. During rainy seasons (June and September), massive freshwater influx is supplied by three major rivers. Whereas Tokyo Bay was previously fringed by a huge area of intertidal flats until the late 1950s, some 20,800 ha of the flats have been reclaimed over past decades (MINISTRY OF TRANSPORT, 2000). The study site has been left from coastal developments to become the largest intertidal flat in Tokyo Bay.

Banzu sandy flat comprises an intertidal area of 7.6 km^2 (760 ha) above the MLLW level. The maximum spring tidal range is about 2.0 m. Bed sediments at the study site are characterized by well-sorted fine sand with a median grain size of 170–190 μm (Figure 2). A preliminary study showed that tidal exchange is the major source of suspended and dis-

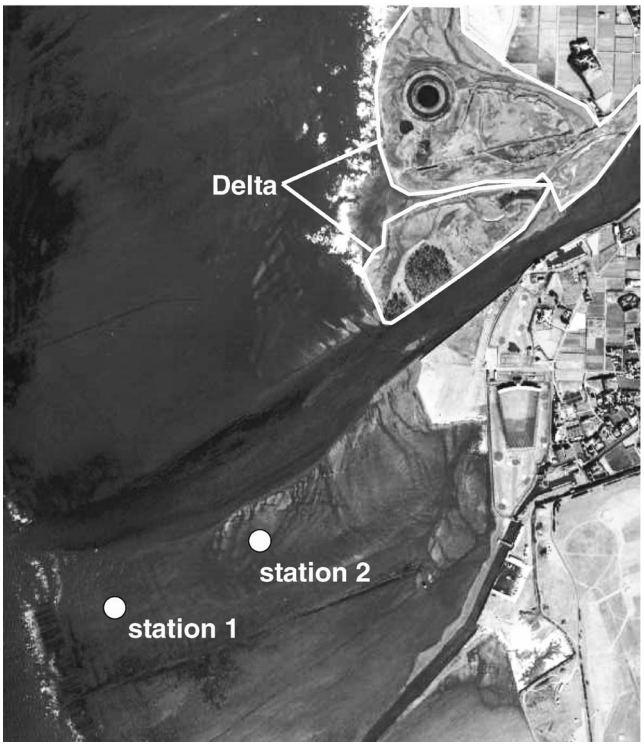

Figure 3. Aerial photo of the study site (Banzu intertidal sand-flat, located off Kisarazu, Chiba Prefecture, Japan).

solved material, although the Obitsu River mouth is located adjacent to the study site (KUWAE *et al.,* 1998). As detailed in the Fluvial Effect subsection in the Results section, freshwater discharge from the adjacent river (Figure 1) directly onto the sandy flat was generally minor during winter (December to February), when the field measurements were performed. Thus, the effects of the river outflow on hydrodynamics and associated sedimentological processes may be assumed negligible in the present analyses. In addition, because of the historical reclamations of the hinterland, there exist almost no marshes or vegetation on Banzu tidal flat except on the delta formed around the mouth of Obitsu River (Figure 3).

The wave climate around the study area is dominated by small wind waves. Tokyo Bay is characterized as a semienclosed estuary, and the bay entrance faces southwest to shelter the study area from the prevailing wind and associated wind waves entering the bay from the Pacific Ocean. Wave heights and periods are limited because of small fetches from the shoreline that comprise two peninsulas and the sand spit at the bay mouth. A number of wave measurements have been performed within the bay. NAGAI *et al.* (2001) estimated a significant wave height $H_{1/3}$ of 0.5 m or less in 88.6% of the waves during 1991–2000. Wave height $H_{1/3}$ of 1.0 m was recorded 0.5% of the time at the Daini-Kaiho Wave Observatory situated in the channel close to the spit at the bay entrance during this decade. They also indicated a significant wave period $T_{1/3}$ to be 5.0 s or more in 1.4% of the waves, suggesting that swells and infragravity waves in the study site are minor.

Methods

A line referred to as transect A–A′ was established near the river mouth, as shown in Figure 1, for the purpose of conducting bathymetric surveys on February 7 and 22, 2000, using a surveyor's level and staff. Instrumentation layout at two monitoring stations, both of which were positioned along transect A–A′, is illustrated in Figure 4. At station 1, water surface elevation was measured using an ultrasonic wave gauge (KENEK Co., Ltd.) mounted at a height of 4.5 m from

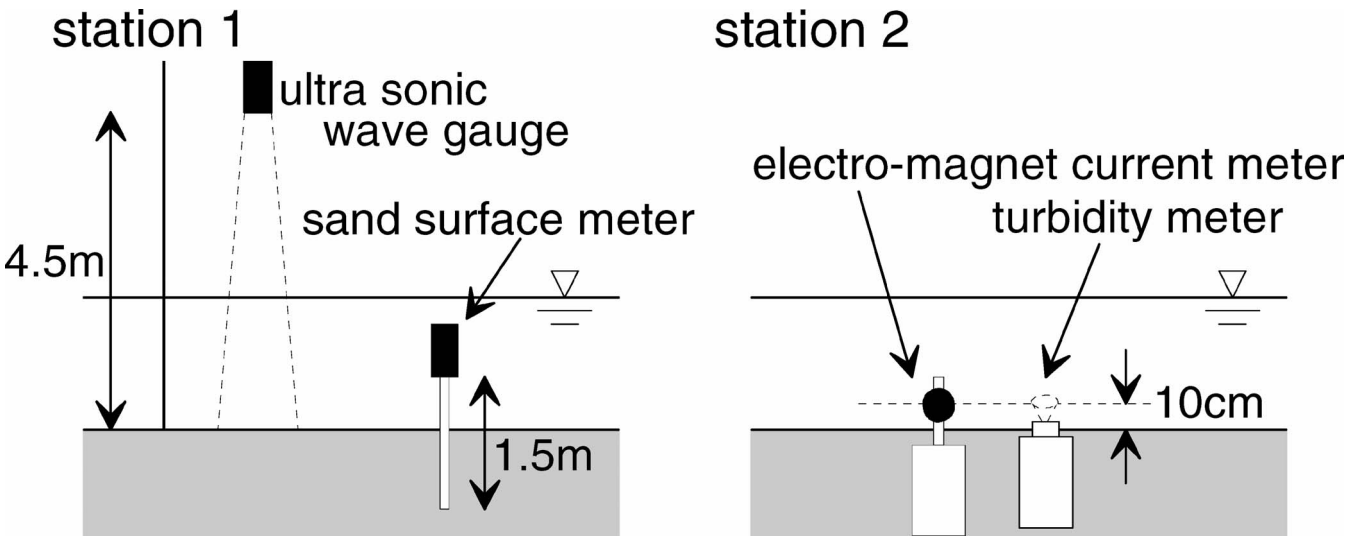

Figure 4. Instrumentation layout (left, station 1; right, station 2).

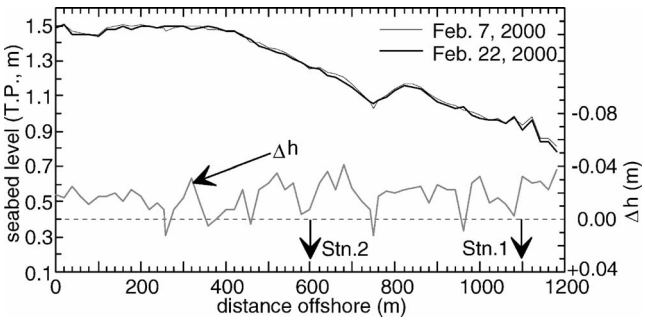

Figure 5. Bottom profiles along transect A–A′ surveyed on February 7 and 22, 2000, and their difference, Δh, along with the positions of stations 1 and 2.

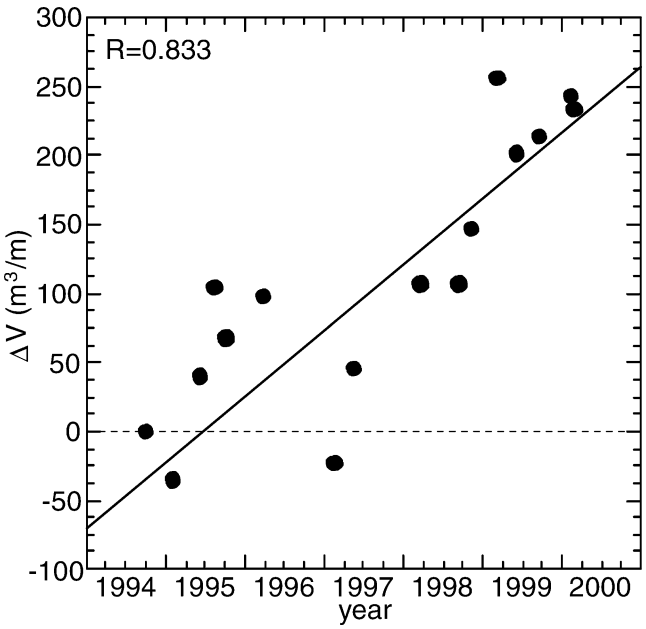

Figure 6. Long-term accumulation evaluated from the bottom survey data along transect A–A′.

the bed at a sampling frequency of 5 Hz, and a photoelectric sand-surface meter (SPM-7, Sanyo Sokki Co., Ltd.) was buried in the bed to monitor bottom elevation at 10-min intervals. The accuracy of the bed elevation measurement is ±5 mm according to the instrument specification. At station 2, an optical backscattering sensor (MTB-16K, Alec Electronics Co., Ltd.) and a three-dimensional electromagnetic current meter (ACM-16M, Alec Electronics Co., Ltd.) were installed to measure suspended sediment concentrations and current velocity at 10 cm above the bed at a frequency of 2 Hz. Fluvial discharge and water level of the Obitsu River were measured at 1-h intervals by the Obitsu Gate Operation Office located at the point 5.6 km upstream from the river mouth. Wind velocity was monitored hourly by the Japan Meteorological Agency at north Kisarazu, about 3.0 km north of the study site. The OBS was calibrated in a laboratory immediately after the deployment with the suspended sediments sampled at the study site. A bucket of about 10 L painted in black and an electrically driven propeller were used to mix the seawater and the sediments. The obtained calibration curves are linear with very small variances, and there is almost no difference in the regression relations calculated with the bed and suspended sediments. These results are considered quite different from those for mudflats, presumably because the sediments are mostly composed of fine sand at the study site.

RESULTS

Short- and Long-Term Morphological Variations

Figure 5 shows bottom profiles surveyed on February 7 and 22, 2000, along transect A–A′ and their difference, Δh. The profile of the sandy tidal flat is found to have a mean slope of about 1:1850, and Δh is very small, ranging from +1 cm to −4 cm. FURUKAWA *et al.* (2000) exhibited a series of bottom topography data of Banzu flat measured along transect A–A′ from October 1994 at intervals of 1–6 months. From their data, long-term variation of the sediment volume along transect A–A′ per unit alongshore length was calculated (Figure 6). The figure indicates that Banzu sandy flat is gradually accreting in the long term at about 45 $m^3/m/y$. By dividing by the length of transect A–A′, 1200 m long, this value can be converted into a profile-averaged long-term accretion rate of 3.8 cm/y. In many tidal wetlands and flats of the world, the accretion rate is only a few millimeters per year (*e.g.,* FREY and BASAN, 1985). Therefore, the accretion rate near the river mouth of Banzu sandy flat is 10 to 30 times greater than those in other studied sites in Europe and America (STEVENSON *et al.,* 1985; FRENCH and SPENCER, 1993; LEONARD *et al.,* 1995; ANDERSON and PEJRUP, 2001).

Figure 7 displays the time series of bed level, *h,* measured at station 1 by SPM-7: (a) original time series (hourly average), (b) 24-h moving averaged bed level representing medium-term fluctuations, (c) difference between (a) and (b), representing short-term fluctuations, and (d) root-mean-square (R.M.S.) of (c) calculated for every 4 hours. As shown in Figures 7a and 7b, the seabed appeared to be eroded by about 8 cm during the first 4 days with small erosions and accumulations, and then gradually recovered to the initial elevation. The magnitude of the short-term erosion occurring on February 8–10 is nearly equivalent to the accretion occurring on February 15–16, as shown in Figures 7c and 7d.

Figure 8 shows time series of tidal elevation averaged for every 30 minutes, the bottom elevation at station 1, and the turbidity (suspended sediment concentrations) averaged for every 10 minutes at station 2. The elevations displayed here are relative to T.P. in meters, where T.P. is the mean lower low water (MLLW) level of Tokyo Bay. The spring-neap-spring tidal cycle and diurnal inequalities are visible in the tidal data. Figures 5 and 8 show that station 1 was mostly submerged over the duration of the deployment, whereas station 2 was exposed during almost every low-water phase. The turbidity (Figure 8) fluctuated in response to the R.M.S. of the bed elevation (Figure 7d), indicating that on February 8 and 9, for instance, high turbidity is observed whenever the

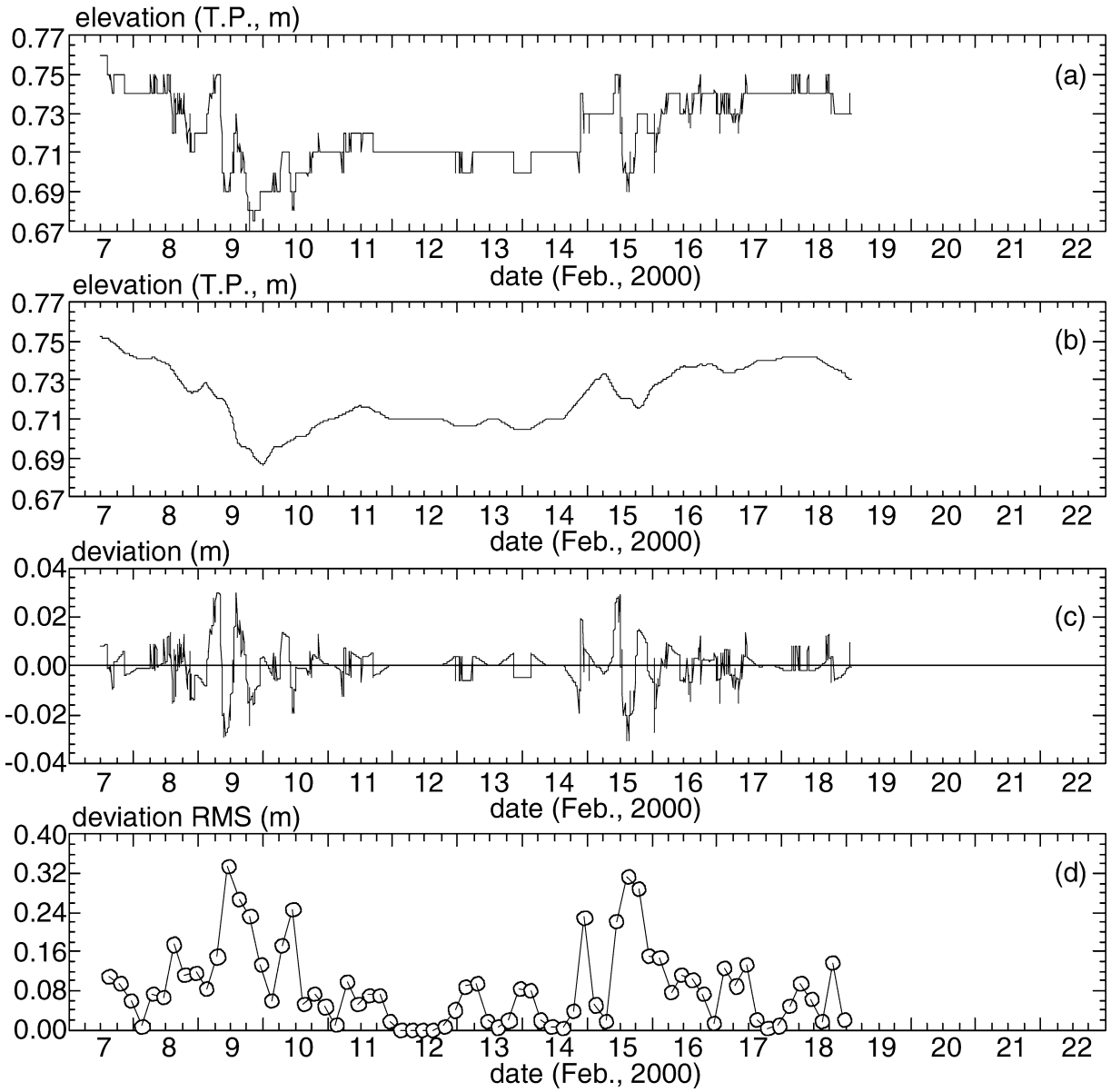

Figure 7. Time series of bed level, *h,* measured at station 1: (a) 1-hour averaged original time series; (b) 24-hour moving averaged bed level; (c) difference between (a) and (b); (d) root-mean-square of (c).

seabed is eroded. In addition, small amounts of erosion and accretion occur with the semidiurnal tidal fluctuations, probably because the wave height, which generally induces the sediment suspensions and resultant bed level variations, varies in response to the tides and has its maximum at high water.

Hydrodynamics

Figure 9 shows significant wave height ($H_{1/3}$) and period ($T_{1/3}$) at station 1 and principal wave directions as estimated from covariance of the current velocity. Figure 10 represents wind velocity vectors at Kisarazu and temporally averaged velocity vectors of horizontal currents and water depth at station 2. Wave conditions are relatively severe at the early stage of the deployment as the wave height reached 0.8–0.9 m with a period of about up to 4 s. Mild conditions prevailed for the next 5 d, followed by medium conditions in the later stage. The principal wave direction is basically from N or NNW, which means that the waves propagated mostly in the alongshore direction, and thus, refraction can be ignored on the sandy flat, although it is significant on sandy beaches.

The wave height fluctuates according to the water depth variation, *i.e.,* tides, as shown in Figures 8 and 9, because $H_{1/3}$ seems to be high during high water but low during low water.

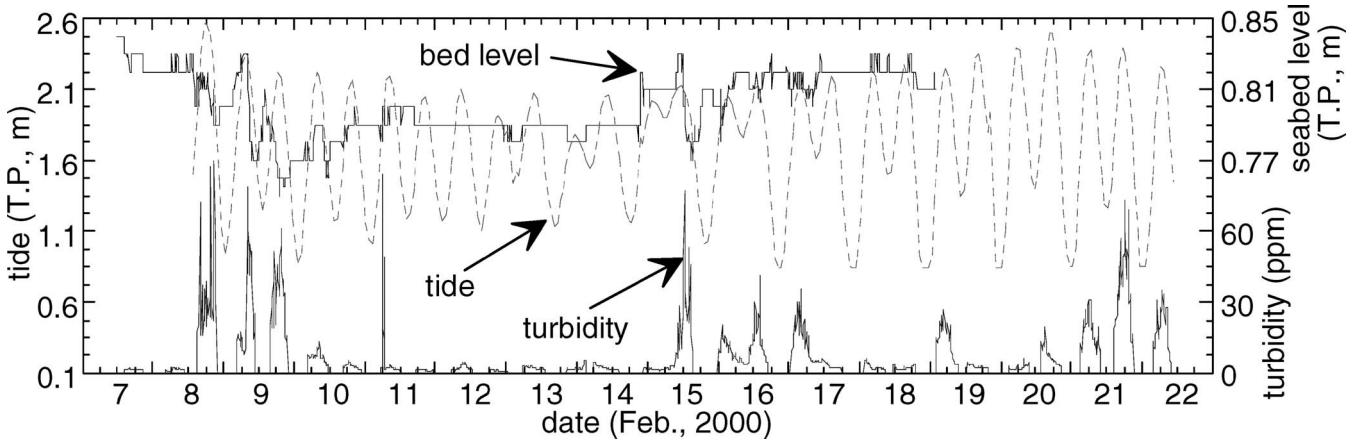

Figure 8. Bottom elevation and tidal elevation at station 1 and turbidity at station 2.

The principal wave directions roughly coincide with the wind directions. Therefore, in order to determine contributions of the wind action and the tidal forcing to the enhancement of wave height, $H_{1/3}$, cross-spectral analysis has been conducted. Figure 11 shows the cross spectra (represented by spectrum, coherence squared, and phase) between (a) significant wave height ($H_{1/3}$) and N–S component of wind velocity ($W_{n\text{-}s}$) and (b) $H_{1/3}$ and η (tide : water depth at station 2). The significant wave height is shown to correlate appreciably with η over broad frequency bands with almost no phase lag. By contrast, coherence between $H_{1/3}$ and the wind velocity is generally small, although it is slightly larger at the lower frequencies. These results demonstrate that $H_{1/3}$ is fluctuating basically in response to the tide, not to the local wind, yet its long-term (at frequency of about 0.01 cycle/h or less) variation is caused mainly by the wind. This result is important because waves (short-period wind waves) are usually believed to be induced by local wind forcing. However, the local water depth is a limiting factor for the development of waves on the extremely shallow intertidal flat.

Next, causes of the variation in the horizontal current velocity are investigated. As shown in Figure 10, the horizontal current velocity appears to vary in the long term in response to the fluctuations of the wind velocity and the wave height. The current field on the sandy flat is also considerably influenced by the tide because the semidiurnal inversions in the current directions occur with the tidal oscillations. As a consequence, the currents on Banzu intertidal flat are simultaneously affected by the wind, the tide, and the waves. Figure 12 shows the cross-spectra between (a) $W_{n\text{-}s}$ and N–S component of horizontal current velocity ($U_{n\text{-}s}$), (b) $H_{1/3}$ and $U_{n\text{-}s}$, and (c) η (tide : depth at station 2) and $U_{n\text{-}s}$. The power spectral density of $U_{n\text{-}s}$ has an intense peak in the vicinity of the semidiurnal period (T = 12 h), although it is relatively low over periods longer than 24 h. The distinct peaks at the semidiurnal period can also be found in the spectra of η and $H_{1/3}$, although there is no visible peak in the wind velocity spectrum. The estimated coherences show that the current variation is obviously correlated with η and $H_{1/3}$ at a period of 12 h. Because the coherence between $U_{n\text{-}s}$ and η is slightly larger than that between $U_{n\text{-}s}$ and $H_{1/3}$, the current velocity fluctuation is considered mainly due to the tide which influences

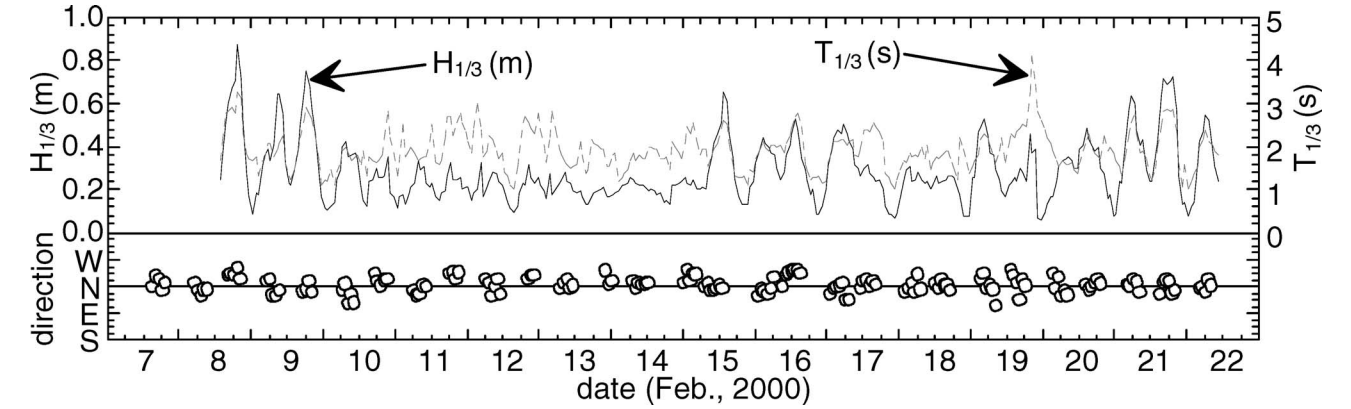

Figure 9. Significant wave height, $H_{1/3}$, and period, $T_{1/3}$, at station 1 and principal wave directions.

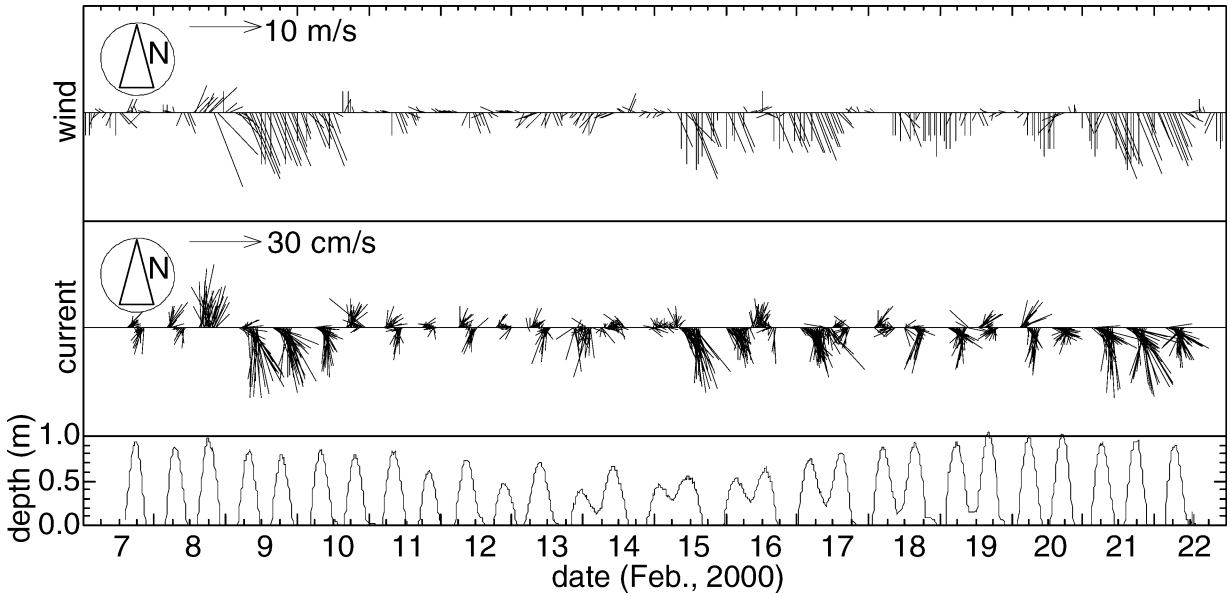

Figure 10. Wind velocities at Kisarazu and current velocities and water depth at station 2.

on the development of the waves. On the other hand, the coherence between $W_{n\text{-}s}$ and $U_{n\text{-}s}$ is high over periods longer than about 24 h, although the longer-period component of $U_{n\text{-}s}$ does not have such a high correlation with the wave height and the tide. Consequently, the wind velocity mainly affects the current field on Banzu sandy flat in the diurnal or longer-period fluctuations, whereas the tide and the waves induce the semidiurnal or shorter-period fluctuations.

Fluvial Effects

Because the study site is situated near the river mouth, influence of the fluvial input from the adjacent Obitsu River must be considered in the analyses. Figure 13 gives a time series of fluvial discharge and water elevations of the Obitsu River monitored at 5.6 km upstream from the river mouth. Although the river discharge during the duration of the measurement fluctuates slightly, it is minor compared with annual variation of the discharge displayed in Figure 14. The tidal elevation is observed to affect the riverine water levels during high tides, although they are generally lower than the riverine water elevations during low tides. Therefore, it is concluded that the freshwater discharge from the adjacent river was presumably small and can be ignored in the present analysis.

DISCUSSION

Bed Shear Stress

The bed shear stresses are calculated to investigate the various mechanism of sediment suspension on Banzu sandy flat. Different methodologies have been proposed to evaluate the bed shear stress in terms of wave-current interaction (*e.g.,* GRANT and MADSEN, 1979; SOULSBY and HUMPHERY, 1990; HUYNH-TANH and TEMPERVILLE, 1991; SOULSBY, 1997), and an approach in which the bed shear stress is estimated using Reynolds stresses calculated from the fluctuating components of the current velocity (DYER and SOULSBY, 1988; FRENCH and CLIFFORD, 1992) is chosen. Assuming that the region in the vicinity of the seabed, where the velocity measurements were performed, is situated in a "constant-shear layer," the bed shear stresses can be calculated using the following equations:

$$\tau_{uw} = -\rho\overline{u'w'}, \tag{1}$$

$$\tau_{vw} = -\rho\overline{v'w'}, \tag{2}$$

$$\tau_b = \sqrt{\tau_{uw}^2 + \tau_{vw}^2}, \tag{3}$$

where $(u', v', w') = (u - U, v - V, w - W)$ is a fluctuating velocity vector, (u, v, w) is a measured current-velocity vector, (U, V, W) is a burst-averaged velocity vector over 15 s of burst intervals, τ_{uw} and τ_{vw} are the vertical components of Reynolds stress in the directions of u and v, ρ is the density of sea water (1025 kg/m^3), and overbars represent an ensemble averaging operator. It might be better to decompose the current velocity into mean flow, wave component, and turbulence. However, that is unfortunately not possible because the sampling frequency of the current meter is too low (2 Hz). One thus must be careful that the bed shear stress τ_b estimated may include wave components.

Figure 15 shows temporal variations of the current bed shear stress τ_b and the turbidity C_s measured at station 2. The turbidity C_s clearly fluctuates in response to τ_b. It is verified that the high turbidities, occurring intermittently on 8, 9, 15, and 21 February, for instance, are generated when higher bed shear stress are observed. Figure 16 supports this

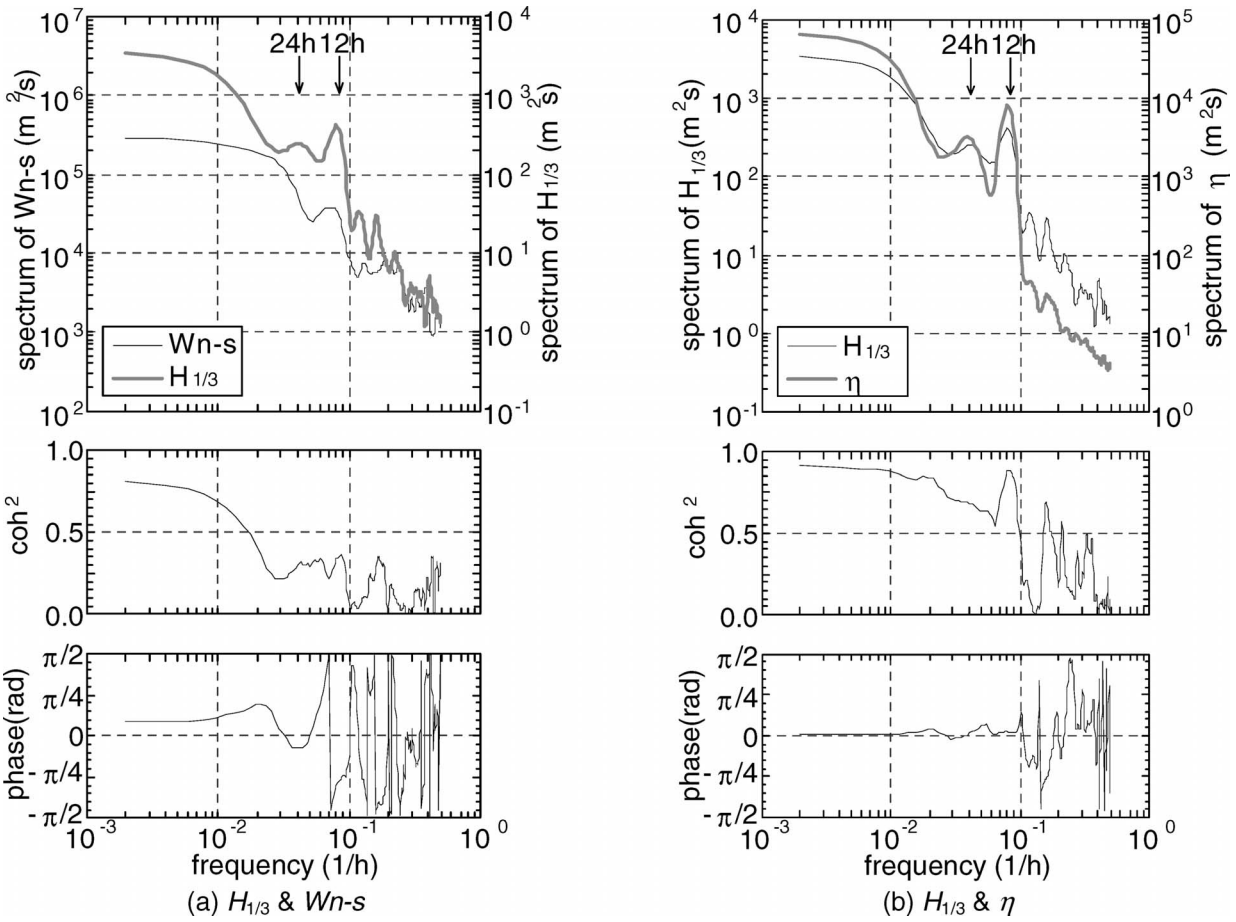

Figure 11. Cross-spectra (a) between significant wave height, $H_{1/3}$, and N–S component of wind velocity, $W_{n\text{-}s}$, and (b) between $H_{1/3}$ and η (tide water depth at station 2).

because the bed shear stress and the turbidity are highly correlated with the correlation coefficient of $R = 0.856$.

Previous studies have shown that modes of sediment transport are related to the Shields parameter, Ψ_m, which is the nondimensional bed shear stress under oscillatory flow with consideration of underlying sediment properties. The relationship between Ψ_m and τ_b is given by

$$\Psi_m = u^{*2}/(\rho_s/\rho - 1)dg = \tau_b/(\rho_s - \rho)dg \quad (4)$$

where u^* is bed friction velocity (m/s), ρ_s and d are the density and median grain size of the bed sediment (2690 kg/m^3 and 0.19 mm), ρ is the seawater density, and g is the gravitational acceleration (9.80 m/s^2). By converting the previously proposed threshold Shields parameters (SHIBAYAMA and HORIKAWA, 1982) into τ_b using equation (4), one obtains $\tau_b \approx 0.2$ N/m^2 for the minimum value for initial generation of bed load, and $\tau_b \approx 0.6$ N/m^2 for the minimum value for transition to suspended load. As shown in Figure 15, whenever the bed sediments are highly suspended, τ_b is much greater than 0.6. Therefore, suspended load dominates on the intertidal sandy flat when high turbidity is measured.

Wave action is well known to have the largest effect on sediment suspension on sandy beaches, particularly in surf zones, and therefore, the correlation between the turbidity and wave energy evaluated from the linear wave theory using the significant wave height is investigated as shown in Figure 17. Note that the waves and current data were separately measured at stations 1 and 2. In spite of this discrepancy, the correlation coefficient R is evaluated to be 0.689. This is considered sufficiently large, although somewhat less than that between τ_b and turbidity.

On the other hand, because hydrodynamics in shallow estuaries is strongly affected by local wind (*e.g.*, WU and TSANIS, 1995), the shear stress induced by the wind action at the water surface, τ_s, is evaluated using the following equation:

$$\tau_s = C_f \rho_a (W_{n\text{-}s}^2 + W_{e\text{-}w}^2) \quad (5)$$

where C_f is the friction coefficient at the sea surface ($= 2.5 \times 10^{-3}$), ρ_a is the atmospheric density ($= 1.2$ kg/m^3), and $(W_{n\text{-}s}, W_{e\text{-}w})$ is a horizontal wind-velocity vector. One can expect that the surface wind stress may be related to the bed stress caused by wind, particularly when water-depth variation is negligible. However, as shown in Figure 18, there is almost no correlation between τ_b and τ_s. This fact again sup-

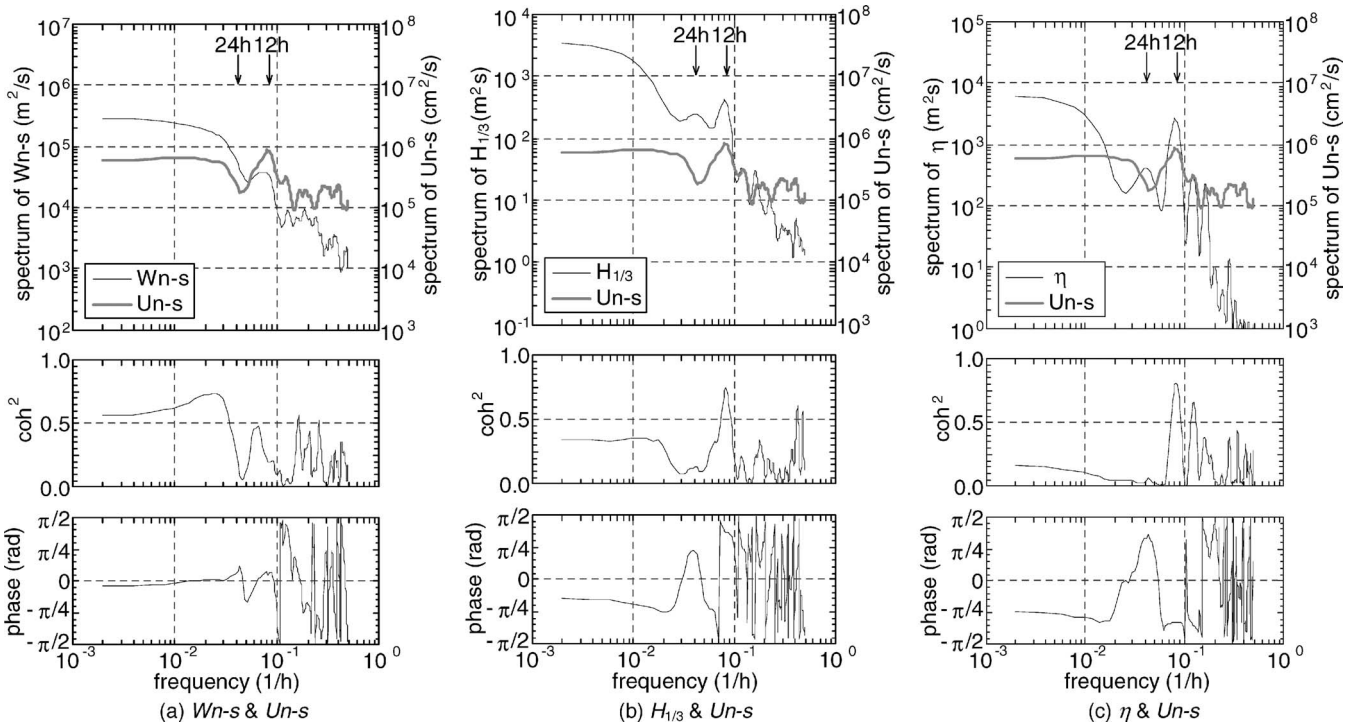

Figure 12. Cross-spectra (a) between $W_{n\text{-}s}$ and N–S component of horizontal current velocity, $U_{n\text{-}s}$, (b) between $H_{1/3}$ and $U_{n\text{-}s}$, and (c) between η and $U_{n\text{-}s}$.

ports the results of the cross-spectral analyses (Figure 12). Consequently, increment of τ_b and the resultant sediment suspension are not directly influenced by wind action, being primarily attributed to the tides and the waves.

Phases of High Concentration of Suspended Sediment

Next, the phases when the high concentrations of suspended sediment are measured are investigated. Conditional samplings are carried out to estimate the ensemble averages (in other words, the phase-averaged pictures) of the wind and current velocities, the tidal elevations, the significant wave height, and the turbidity. The condition is defined here as the turbidity exceeding 40 ppm (*i.e.,* bed shear stress to exceed about 3.5 N/m²). The conditional samplings (*e.g.,* YUAN and MOKHTARZADEH-DEHGHAN, 1994) are executed to obtain the ensemble averages for five cases of high concentrations mea-

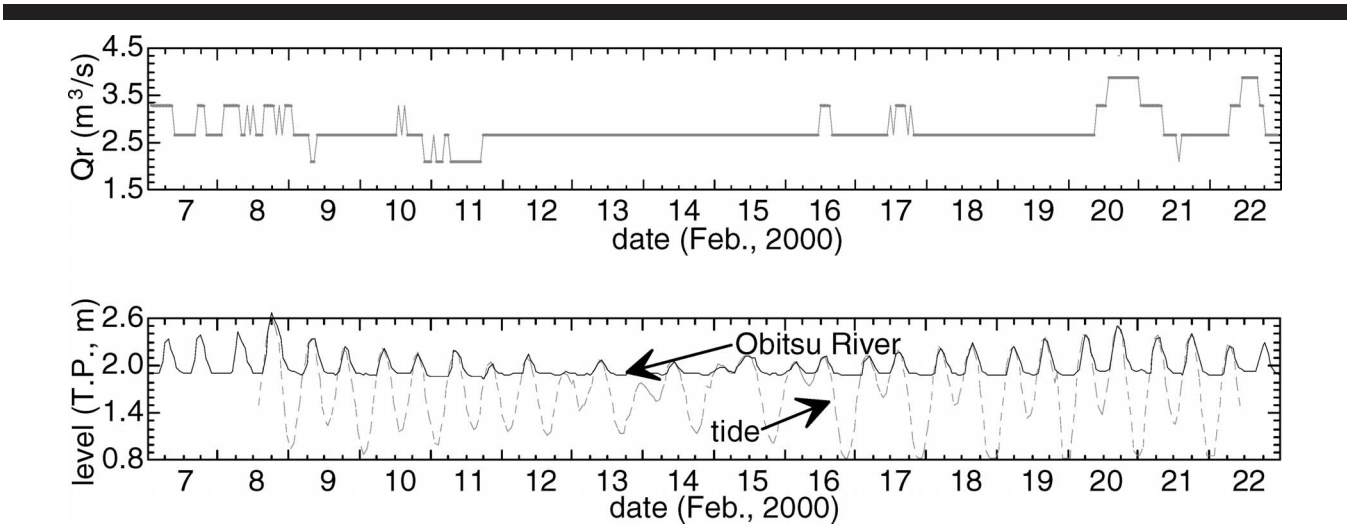

Figure 13. Discharge and water level of the Obitsu River measured at 5.6 km upstream from the river mouth. Upper panel: River discharge. Lower panel: Tidal elevation at station 2 and river water level.

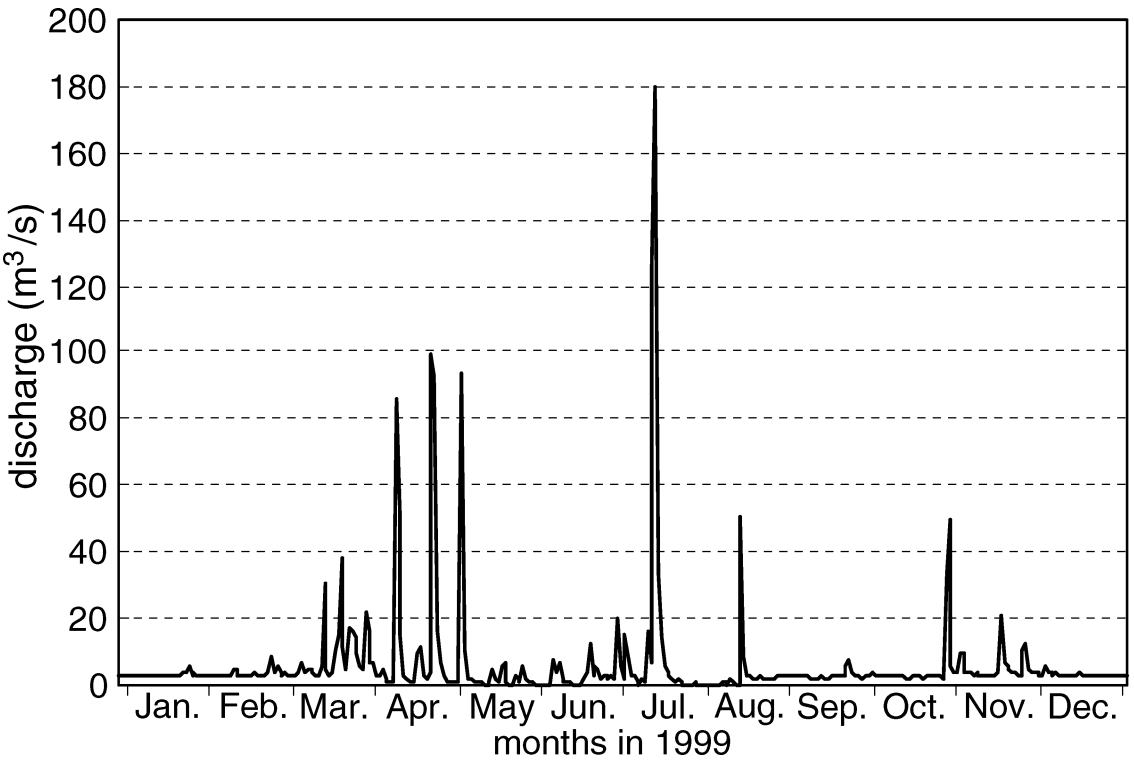

Figure 14. Annual variation of the Obitsu River discharge measured at 5.6 km upstream from the river mouth in 1999.

sured at 2100 on February 8, 0820 and 1940 on February 9, 1240 on the 15th, and 1810 on the 21st. The estimated ensemble averages are shown in Figure 19, in which the phase of high turbidity is adjusted to the elapsed time $t = 0$ h for each case. The current velocity, the wind velocity, and the bed shear stress apparently have highest values near the phase of the high turbidity. In contrast, the peak phases of the wave height and the tidal elevation do not correspond to the phase of high turbidity. The turbidity is found high during ebb tide, which begins at around $t = -1.5$ h, and becomes the highest at the phase between the high slack and the mean water, 1.5 h after the high slack water.

Intertidal flats are reported quite sensitive to action of wind-induced waves because they are extremely shallow, which favors the generation of high bed shear stresses that promote sediment resuspension (FREEMAN *et al.*, 1994). In other words, a net transport of suspended sediments may be significantly dependent on wind speed and direction, as suggested by PEJRUP (1986), CHRISTIE *et al.* (1999), and BASSOULLET *et al.* (2000). The wave height has its peak at the high

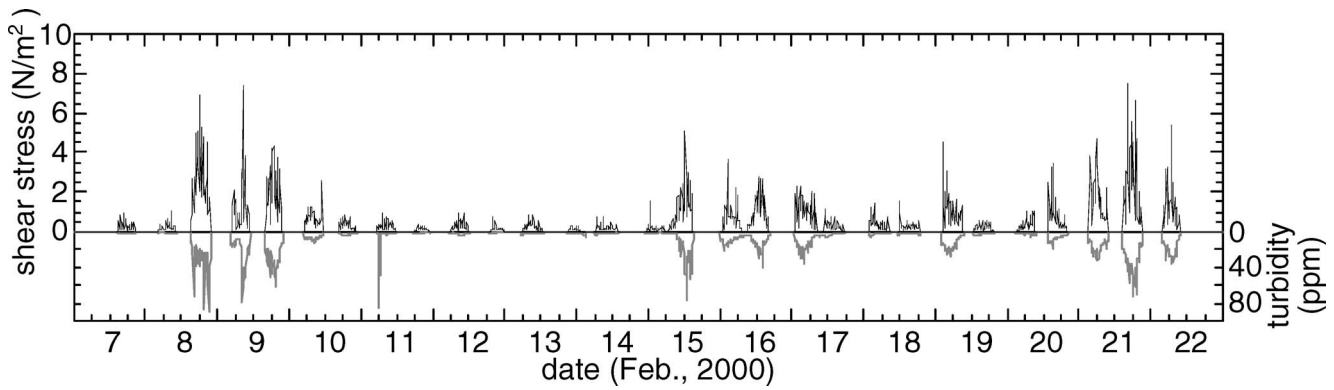

Figure 15. Bed shear stress (solid line) and turbidity (dotted line) at station 2.

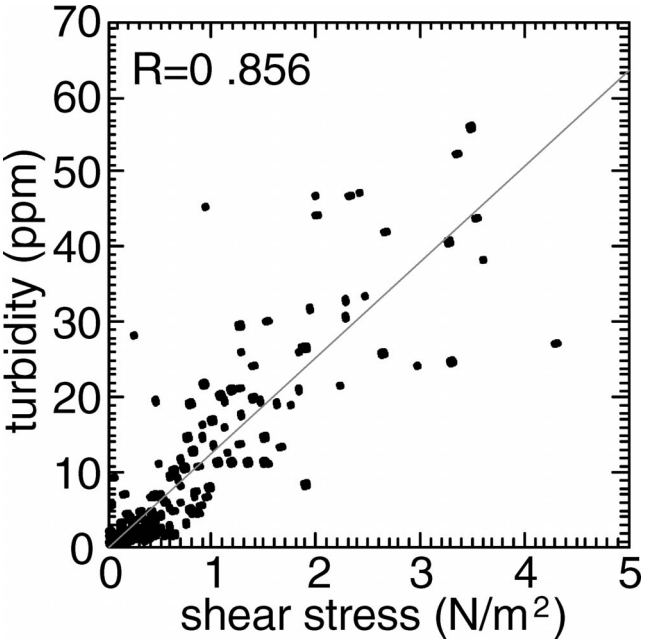

Figure 16. Correlation between bed shear stress, τ_b, and turbidity.

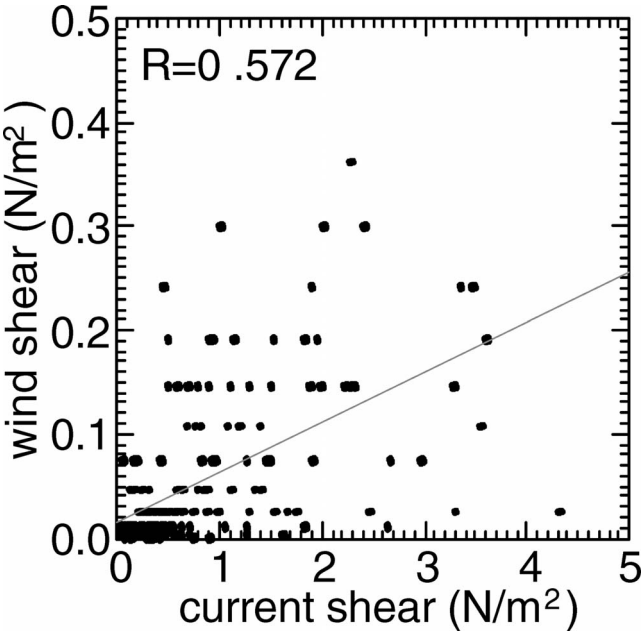

Figure 18. Correlation between bed shear stress and wind shear stress at surface.

slack phase because it fluctuates in response to the tide as shown in Figure 11b. If only the waves are predominant in generating the bed shear stress as in surf zones, the highest turbidity may not appreciably lag behind the high-water phase. In general, tidal current velocities become largest between high slack and low slack phases during flooding and ebbing. If the semidiurnal tidal component is dominant as in Tokyo Bay, the maximum tidal velocities, as well as resultant bed shear stresses, appear at 3 h and 9 h after the low slack. However, the estimated phase of high turbidity in Figure 19 is found at 1.5 h after the phase of the high water and the maximum wave height, and at 1.5 h before the tidal current velocity and the bed shear stress become maximal. This dis-

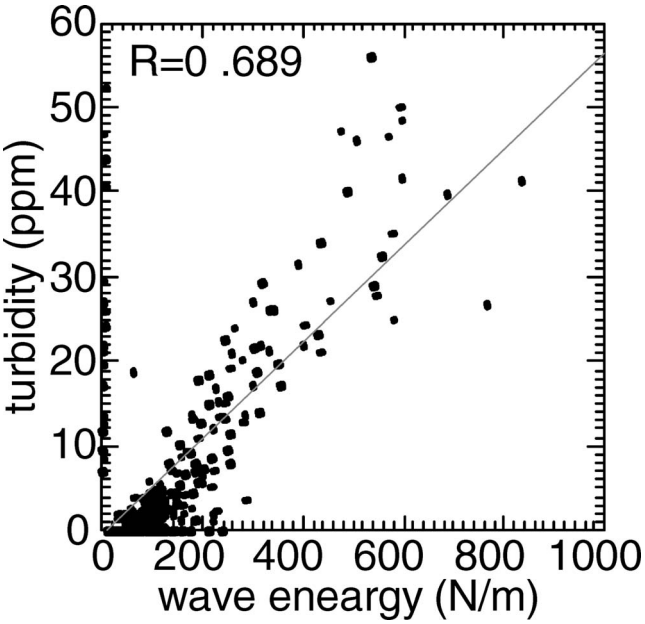

Figure 17. Correlation between wave energy and turbidity.

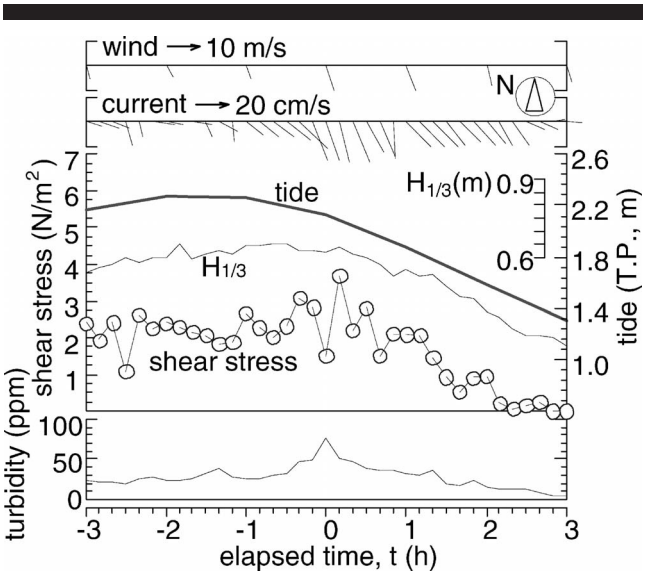

Figure 19. Ensemble averaged wind velocities, current velocities, tidal elevation, significant wave height, bed shear stresses, and suspended sediment concentrations calculated with conditional sampling when the turbidity is in excess of 40 ppm.

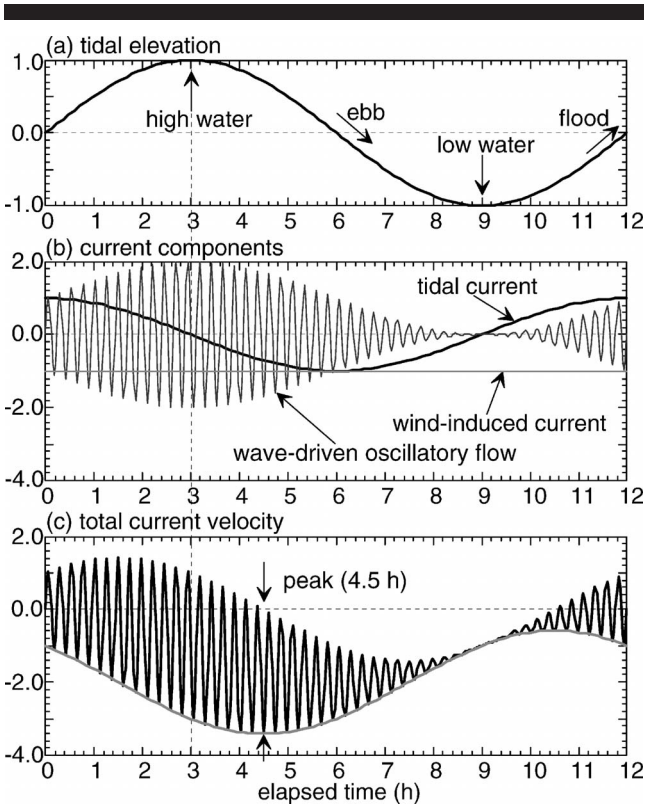

Figure 20. Conceptual illustration of the current generation on Banzu intertidal flat: (a) tidal elevation; (b) velocities of wind-induced current, tidal current, and wave-driven oscillatory flow; and (c) resultant total current velocity. Tide is assumed to consist of only the semidiurnal component. High water and low water are set here to be at 3 h and 9 h, respectively.

crepancy suggests that combined wave and current interaction is essential to generation of the bed shear stress as conceptually illustrated in Figure 20. If the contributions of waves and currents to produce the bed shear stress are equivalent (*i.e.,* the amplitude of tidal currents and wave orbital velocities are assumed to be the same), and the direction of wind coincides with that of ebb tidal currents, the total velocity has the maximum value during ebbing at the phase of 1.5 h after the high water, as shown in Figure 20c. When the amplitudes of tidal currents and wave orbital velocities are not the same, the phase of high turbidity is evidently different from that shown in Figure 19. When wind blows in the direction of flood tidal currents, the maximum concentration appears at a phase 1.5 h before the high water. This result supports the importance of a combination of waves, tidal currents, and wind-induced currents to hydrodynamics, associated sediment transport, and topography variations on the sandy tidal flat.

CONCLUSIONS

The results of a 16-day field measurement on hydrodynamics, sediment suspension and topography variations and a 6-year series of bed-profile surveys demonstrate that an estuarine intertidal sandy flat in the semienclosed Tokyo Bay, Japan, has a morphological process consisting of long-term gradual accretion, episodic erosions, and subsequent accumulations. The long-term accretion rate is estimated to be only about 3.8 cm/y on the basis of the surveyed data, whereas bed elevation varies by approximately 8 cm during the short-term measurement conducted in 2000, when fluvial discharge can be ignored and relatively severe wave condition appears as significant wave height exceeds 0.8 m during the deployment. Episodic erosion and subsequent gradual accretion are significant for the short-term morphological processes. Modes of bottom sediment movement during the measurement are examined using the Shields parameter. Erosion occurs in response to generation of high concentrations of suspended sediments at phases between the high slack water and the mean water during ebb, when the combined wave and current interactions are predominant. On Banzu sandy flat, a key mechanism to produce high turbidity is considered to be the combination of high waves, strong ebb-tidal current, and acceleration as a result of wind blowing in the direction of ebb-tidal currents. By contrast, the bed elevation tends to accrete immediately after the erosion episodes as the wave height decreases. The waves are observed to develop and attenuate in response to the tidal elevations, suggesting that the short-term cyclic morphological processes also are attributed to the tides.

ACKNOWLEDGMENTS

The author is grateful to Dr. Keita Furukawa of National Institute for Land and Infrastructure Management, Japan, for his cooperation in making available the long-term topography data surveyed on Banzu tidal flat. Acknowledgement is made to Dr. Tomohiro Kuwae of Port and Airport Research Institute (PARI), Japan, Dr. Munemasa Nomura of Tohoku University, Japan, Mr. Tsuyoshi Nakashima of Ministry of Land, Infrastructure and Transport, Japan, and Mr. Tomoaki Fujino of Toyo Construction Co., Ltd., Japan, for their earnest help with the field measurements. The author would like to express sincere appreciation to Dr. Yoshiaki Kuriyama and Dr. Kazumasa Katoh of PARI, Professor Terry Healy of the University of Waikato, New Zealand, and an anonymous reviewer for their thorough and constructive comments on the manuscript. This study was partially supported by Sumitomo Foundation.

LITERATURE CITED

AMOS, C.L.; VAN WAGONER, N.A., and DABORN, G.R., 1998. The influence of subaerial exposure on the bulk properties of fine-grained intertidal sediment from Minas Basin, Bay of Fundy. *Estuarine, Coastal and Shelf Science,* 27, 1–13.

ANDERSEN, T.J., 2001. Seasonal variation in erodibility of two temperate, microtidal mudflats. *Estuarine, Coastal and Shelf Science,* 53, 1–12.

ANDERSEN, T.J., and PEJRUP, M., 2001. Suspended sediment transport on a temperate, microtidal mudflat, the Danish Wadden Sea. *Marine Geology,* 173, 69–85.

AUSTEN, I.; ANDERSEN, T.J., and EDELVANG, K., 1999. The influence of benthic diatoms and invertebrates on the erodibility of an intertidal mudflat, the Danish Wadden Sea. *Estuarine, Coastal and Shelf Science,* 49, 99–111.

BAKKER, J.P.; DE LEEUW, J.; DIJKEMA, K.S.; LEENDERTSE, P.C.; PRINS, H.H.T., and ROZEMA, J., 1993. Salt marshes along the coast of the Netherlands. *Hydrobiologia,* 265, 73–95.

BASSOULLET, PH.; LE HIR, P.; GOULEAU, D., and ROBERT, S., 2000. Sediment transport over an intertidal mudflat: field investigations and estimation of fluxes within the "Baie de Marennes-Oleron" (France). *Continental Shelf Research,* 20, 1635–1653.

CHRISTIE, M.C.; DYER, K.R., and TURNER, P., 1999. Sediment flux and bed level measurements from a macro tidal mudflat. *Estuarine, Coastal and Shelf Science,* 49, 667–688.

DALRYMPLE, R.W.; MAKINO, Y., and ZAITLIN, B.A., 1991. Temporal and spatial pattern of rhythmic deposition on mudflats in the macrotidal Cobequid Bay-Salmon River estuary, Bay of Fundy, Canada. *In*: SMITH, D.G.; REINSON, G.E.; ZAITLIN, B.A., and RAHMANI, R.A. (eds), *Clastic Tidal Sedimentology,* Canadian Society for Petroleum Geology Memoirs, 16, pp. 137–160.

DYER, K.R. and SOULSBY, R.L., 1988. Sand transport on the continental shelf. *Annual Review of Fluid Mechanics,* 20, 295–324.

DYER, K.R.; CHRISTIE, M.C.; FEATES, N.; FENNESSY, M.J.; PEJRUP, M. and VAN DER LEE, M., 2000. An investigation into processes influencing the morphodynamics of an intertidal mudflat, the Dollard Estuary, the Netherlands: I. Hydrodynamics and suspended sediment. *Estuarine, Coastal and Shelf Science,* 50, 607–625.

FERNS, P.N., 1983. Sediment mobility in the Severn Estuary and its influence upon the distribution of shorebirds. *Canadian Journal of Fisheries and Aquatic Science,* 40 (Supp 1), 331–340.

FREEMAN, D.P.; COATES, L.E.; OCKENDEN, M.C.; ROBERTS, W., and WEST, J.R., 1994. Cohesive sediment transport on an inter-tidal zone under combined wave-tidal flow. *Netherlands Journal of Aquatic Ecology,* 28 (3–4), 283–288.

FRENCH, J.R. and CLIFFORD, N.J., 1992. Characteristics and event-structure of near-bed turbulence in a macrotidal salt-marsh channel. *Estuarine, Coastal and Shelf Science,* 34, 49–69.

FRENCH, J.R. and SPENCER, T., 1993. Dynamics of sedimentation in a tide-dominated backbarrier salt marsh, Norfork, UK. *Marine Geology,* 110, 315–331.

FREY, R.W. and BASAN, P.B., 1985. Coastal salt marshes, *In*: DAVIS, R.A. (ed.), *Coastal Sedimentary Environments*. New York: Springer-Verlag, pp. 225–289.

FURUKAWA, K.; FUJINO, T.; MIYOSHI, T.; KUWAE, T.; NOMURA, M.; HAGIMOTO, Y., and HOSOKAWA, Y., 2000. Topographical change on tidal flats' case study on Banzu natural tidal flat and Nishiura constructed tidal flat. Technical Note of the Port and Harbour Research Institute, 965. Yokosuka, Japan: PHRI, pp. 1–30. (in Japanese)

GRANT, W.D. and MADSEN, O.S., 1979. Combined wave and current interaction with a rough bottom. *Journal of Geophysical Research,* 84, 1797–1808.

HOUWING, E.-J., 2000. Morphodynamic development of intertidal mudflats: consequences for the extension of the pioneer zone. *Continental Shelf Research,* 20, 1735–1748.

HUYNH-TANH, S. and TEMPERVILLE, A., 1991. A numerical model of the rough turbulent boundary layer in combined wave and current interaction, *In*: SOULSBY, R.L., and BETTEES, R. (eds), *Euromech 262 Sand Transport in Rivers, Estuaries and the Sea*. Rotterdam, The Netherlands: Balkema.

KAKINO, J., 2000. Dispersal of Japanese littleneck clam Ruditapes philippinarum (Adams and Reeve) in relation to changes of bottom level due to wave action on Banzu tidal flat, Tokyo Bay. *Fisheries Engineering,* 37(2), 115–128.

KIRBY, R.; BLEAKLEY, R.J.; WEATHERUP, S.T.C.; RAVEN, P.J., and DONALDSON, N.D., 1993. Effect of episodic events on tidal mudflat stability, Ardmillan Bay, Strangford Lough, Northern Ireland. *In*: MEHTA, A.J. (ed.), *Nearshore and Estuarine Marine Cohesive Sediment Transport, Coastal and Estuarine Studies,* 42, Washington, DC: AGU, pp. 378–392.

KUWAE, T.; HOSOKAWA, Y., and EGUCHI, N., 1998. Dissolved inorganic nitrogen cycling in Banzu intertidal sand-flat, Japan. *Mangroves and Salt Marshes,* 2, 167–175.

LE HIR, P.; ROBERTS, W.; CAZAILLET, O.; CHRISTIE, M.; BASSOULLET, P., and BACHER, C., 2000. Characterization of intertidal flat hydrodynamics. *Continental Shelf Research,* 20, 1433–1459.

MINISTRY OF TRANSPORT, SECOND PORT CONSTRUCTION BUREAU, 2000. *The Environmental Data Book in Tokyo Bay,* Yokohama, Japan: Ministry of Transport, 47p. (in Japanese)

MITCHENER, H.; TORFS, H., and WHITEHOUSE, R., 1996. Erosion of mud/sand mixtures. *Coastal Engineering,* 29, 1–25.

NAGAI, N.; SATO, K.; SUGAHARA, A., and KAWAGUCHI, K., 2001. Annual report on nationwide ocean wave information network for ports and harbours (NOWPHAS 2000), Technical Note of the Port and Harbour Research Institute, 988. Yokosuka, Japan: PHRI, 402p. (in Japanese)

O'BRIEN, D.J.; WHITEHOSE, R.J.S., and CRAMP, A., 2000. The cyclic development of a macrotidal mudflat on varying timescales. *Continental Shelf Research,* 20, 1593–1619.

PATERSON, D.M., 1989. Short-term changes in the erodibility of intertidal sediments related to the migratory behavior of epipelic diatoms. *Limnology and Oceanography,* 34, 223–234.

PEJRUP, M., 1986. Parameters affecting fine-grained suspended sediment concentrations in a shallow micro-tidal estuary, Ho Bugt. *Estuarine, Coastal and Shelf Science,* 22, 241–254.

RHOADS, D.C. and BOYER, L.F., 1982. The effects of marine benthos on physical properties of sediments: a successional perspective, *In*: MCCALL, P.L., and TEVESZ, M.J.S. (eds.), *Animal–Sediment Relations: the Biogenic Alteration of Sediments*. New York: Plenum Press, pp. 3–52.

SHIBAYAMA, T. and HORIKAWA, K., 1982. Sediment transport and beach transformation. *Proceedings of the 18th Coastal Engineering Conference,* ASCE, pp. 1439–1458.

SOULSBY, R.L., 1997. *Dynamics of Marine Sands: A Manual for Practical Applications,* London: Thomas Telford, 250p.

SOULSBY, R.L. and HUMPHERY, J.D., 1990. Field observations of wave–current interaction at the sea bed, *In*: TORMAN, A., and GUDMESTAD, O.T. (eds), *Water Wave Mechanics*. The Netherlands: Kluwer Academic Publishers, pp. 413–428.

STEVENSON, J.C.; KEARNEY, M.S., and PENDLETON, E.C., 1985. Sedimentation and erosion in a Chesapeake Bay brackish salt marsh system. *Marine Geology,* 80, 37–59.

TALKE, S.A. and STACEY, M.T., 2003. The influence of oceanic swell on flows over an estuarine intertidal mudflat in San Francisco Bay. *Estuarine, Coastal and Shelf Science,* 58, 541–554.

TEISSON, C.; OCKENDEN, M.C.; LE HIR, P.; KRANENBURG, C., and HAMM, L., 1993. Cohesive sediment transport processes. *Coastal Engineering,* 21, 129–162.

TORFS, H.; MITCHENER, H.; HUYSENTRUYT, H., and TOORMAN, E., 1996. Settling and consolidation of mud/sand mixtures. *Coastal Engineering,* 29, 27–45.

VAN DER LEE, W.T.B., 2000. Temporal variation of floc size and settling velocity in the Dollard estuary. *Continental Shelf Research,* 20, 1495–1511.

WEST, M.S. and WEST, J.R., 1991. Spatial and temporal variations in intertidal zone properties in the Severn Estuary, UK, *In*: ELLIOT, M., and DUCROTOY, J.P. (eds.), *Estuaries and Coasts*. Fredensborg: Alson and Alson, pp. 25–30.

WHITEHOSE, R.J.S. and MITCHENER, H.J., 1998. Observations of morphodynamic behaviour of an intertidal mudflat at different timescales, *In*: BLACK, K.S.; PATERSON, D.M., and CRAMP, A. (eds.), *Sedimentary Processes in the Intertidal Zone,* 139, 255–271.

WIDDOWS, J.; BRINSLEY, M. and ELLIOTT, M., 1998. Use of in situ flume to quantify particle flux (biodeposition rates and sediment erosion) for an intertidal mudflat in relation to changes in current velocity and benthic macrofauna, *In*: BLACK, K.S.; PATERSON, D.M., and CRAMP, A. (eds.), *Sedimentary Processes in the Intertidal Zone,* 139, 85–97.

WILLIAM, H.F.L. and HAMILTON, T.S., 1995. Sedimentary dynamics of an eroding tidal marsh derived from stratigraphic records of 137Cs fallout, Fraser Delta, British Columbia, Canada. *Journal of Coastal Research,* 14(4), 1145–1156.

WU, J. and TSANIS, I.K., 1995. Numerical study of wind-induced water currents. *Journal of Hydraulic Engineering,* 121, 388–395.

YUAN, Y.M. and MOKHTARZADEH-DEHGHAN, M.R., 1994. A comparison study of conditional sampling methods used to detect coherent structures in turbulent boundary layers. *Physics of Fluids,* 6, 2038–2057.